

Available online at www.sciencedirect.com

ScienceDirect

journal homepage: www.elsevier.com/locate/radcr

Case Report

A rare case of a primary central nervous system neuroblastoma mimicking a trigeminal schwannoma in an adult[☆]

Bui Quang Huynh, MD^{a,1}, Nguyen Duy Hung, MD^{a,b,1}, Nguyen Ha Khuong, MD^b,
 Nguyen Ngoc Anh, MD^b, Nguyen Minh Duc, MD^{c,*}

^a Department of Radiology, Viet Duc Hospital, Hanoi, Vietnam

^b Department of Radiology, Hanoi Medical University, Hanoi, Vietnam

^c Department of Radiology, Pham Ngoc Thach University of Medicine, 2 Duong Quang Trung Ward 12 Distric, Ho Chi Minh City, 700000, Vietnam

ARTICLE INFO

Article history:

Received 2 February 2023

Revised 3 April 2023

Accepted 7 May 2023

Keywords:

Primary central nervous system
 neuroblastoma

Trigeminal schwannoma

Cerebellopontine angle

ABSTRACT

Neuroblastoma is a malignant extra-cranial tumor that frequently arises in the pediatric population aged <5 years but is rare in adults. Only a few cases of primary central nervous system neuroblastoma (PCN-NB) have been documented, with most occurring in young patients. In this article, we report an adult case with a PCN-NB in the cerebellopontine angle-middle cranial fossa region that mimicked another neoplasm. We also discuss the magnetic resonance imaging features and pathological characteristics of PCN-NB and differential diagnosis strategies.

© 2023 The Authors. Published by Elsevier Inc. on behalf of University of Washington.

This is an open access article under the CC BY-NC-ND license

(<http://creativecommons.org/licenses/by-nc-nd/4.0/>)

Introduction

Neuroblastoma is the most common extra-cranial neoplasm in children under 5, accounting for 8%-10% of all malignancies in pediatric patients. Neuroblastoma often originates in nerve tissue of the adrenal gland or sympathetic nerve ganglia. Intracranial neuroblastoma primarily occurs in cases with metastasis from the extra-cranial tumor, a so-called metastatic intracranial neuroblastoma. However, pri-

mary central nervous system (CNS) neuroblastoma (PCN-NB) is rare [1]. PCN-NB was originally called a primitive neuroectodermal tumor, but The World Health Organization (WHO) discontinued that term in 2016. It has the International Classification of Diseases for Oncology (ICD-O) code 9500/3, a neuroepitheliomatous neoplasms category under neuronal and para-neuronal tumors [2,3].

Previous studies imprecisely classified PCN-NB with medulloblastoma, undifferentiated ependymoma, and sarcoma. Therefore, they did not provide representative and

[☆] Competing Interests: The authors have declared that no competing interests exist.

* Corresponding author.

E-mail address: bsnguyenminhduc@pnt.edu.vn (N.M. Duc).

¹ These authors contributed equally to this article as co-first authors.

<https://doi.org/10.1016/j.radcr.2023.05.028>

1930-0433/© 2023 The Authors. Published by Elsevier Inc. on behalf of University of Washington. This is an open access article under the CC BY-NC-ND license (<http://creativecommons.org/licenses/by-nc-nd/4.0/>)

reliable statistics for PCN-NB. Consequently, knowledge about this cancer is limited [4,5]. To our knowledge, only a few PCN-NB cases have been reported, with an incidence of 0.12 cases per 1,000,000 population annually. Most cases involve pediatric patients and only sporadically adults [1,2,4,6,7]. Lu et al. [2] analyzed the Surveillance, Epidemiology, and End Results (SEER) program data in 2020, finding that 40.7% of patients were aged 1-9 years and only 8.2% were aged >40 years. Two criteria are sufficient to establish a PCN-NB diagnosis: (1) pathological imaging conforming to neuroblastoma and (2) no systemic neuroblastoma in another location.

PCN-NB's clinical symptoms are nonspecific and primarily depend on the tumor's location, including headache, neuro-deficit symptoms, seizure, and even altered consciousness in cases with sudden intra-tumoral hemorrhage [6]. Some studies indicate that PCN-NB often arises in the supratentorial brain parenchyma [6,7]. Tietze et al. [9] examined 25 PCN-NB patients, finding that the most frequent primary location was the frontal lobe (72%), followed by the parietal lobe (44%), temporal lobe (36%), and basal ganglia (32%). However, no reliable and specific imaging characteristic has been found to differentiate PCN-NB from other malignant brain neoplasms. Computed tomography and magnetic resonance imaging (MRI) of intracranial PCN-NBs often show a large lobulated mass with a heterogeneous structure comprising intratumoral cystic degeneration, calcification, and hemorrhage, with a moderate-to-strong enhancement of solid components and frequent

peritumoral edema [6,9]. In addition, PCN-NBs manifest several malignant neoplasm aspects, such as low apparent diffusion coefficient (ADC) values due to restricted water molecule diffusion in high cellularity lesions, rapid expansion, and intratumoral hemorrhage [6,9,10].

In this article, we report an adult case with a PCN-NB in the cerebellopontine angle-middle cranial fossa region that was surgically removed to provide the histopathological PCN-NB finding.

Case report

A previously healthy 29-year-old female initially presented with a history of headaches unresponsive to treatment for 3 months. The physical examination showed that the patient was alert, fully oriented, and had no signs of focal neurological deficits. She had no motor or sensory deficits.

An MRI with contrast was performed to help evaluate the findings. It revealed a sizeable extra-cranial mass in the left cerebellopontine angle, measuring approximately 41×18 mm in diameter, extending into Meckel's cave and the middle cranial fossa. The three-dimensional (3D) constructive interference in steady state (CISS) sequence showed a marked mass effect, characterized by compression of the left middle cerebellar peduncle, pons, and fourth ventricle without hydro-

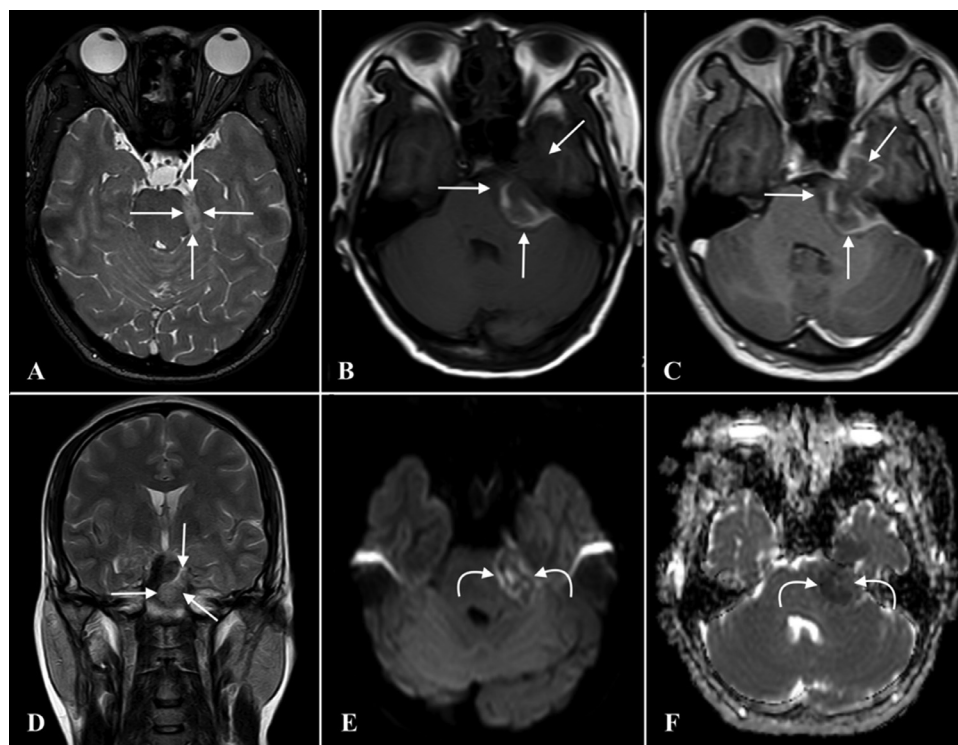


Fig. 1 – The preoperative brain MRI. It showed a left cerebellopontine angle extra-cranial lesion extending into Meckel's cave and the middle cranial fossa. (B) Peripheral hyperintensity and central hypointensity in axial postcontrast T1W axial images corresponding to peripheral hypointensity and central hyperintensity in T2W (A) axial and (D) coronal images (straight arrow). (C) Postgadolinium T1W images show heterogeneous contrast enhancement with a solid enhancing component in the middle cranial fossa. Heterogeneous diffusion restriction areas are observed on the (E) DWI and (F) ADC map (curved arrow).

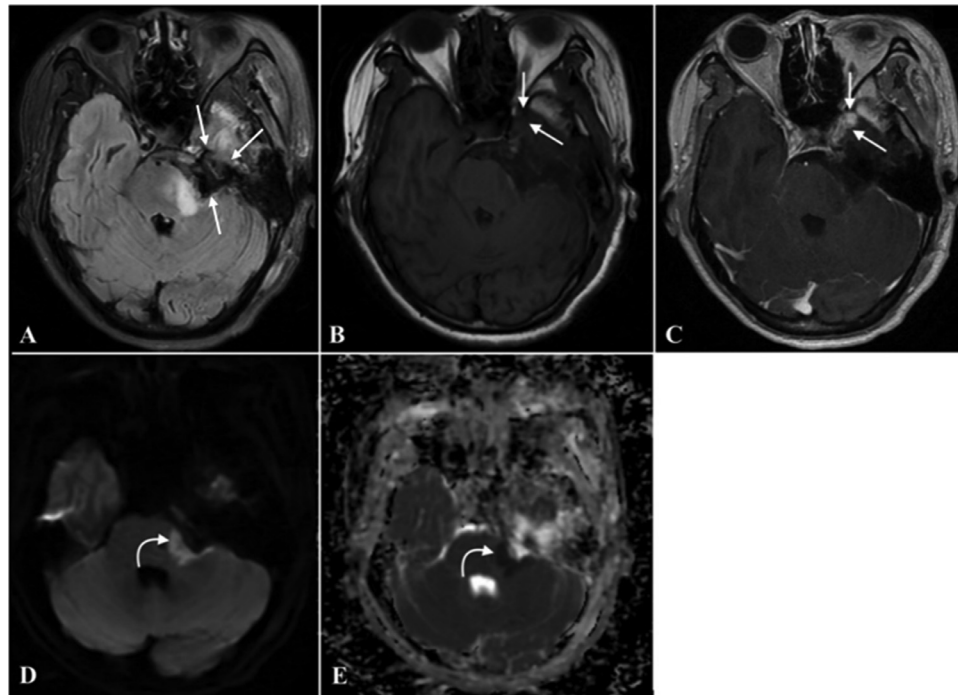


Fig. 2 – MRI brain images at 4 days postsurgery. (A) An axial fluid-attenuated inversion recovery image shows an enlargement of the subarachnoid space in the left cerebellopontine angle (straight arrows). Comparison of (B) pre- and (C) postcontrast T1W images shows enhancing residual tumor in lateral cavernous sinus wall (straight arrows). (D) An axial DWI with corresponding (E) ADC map shows diffusion restriction in the left middle cerebellar peduncle and pons due to cerebral ischemia adjacent to the tumor bed area (curved arrows).

cephalus. The lesion was closed to the lateral cavernous sinus wall but did not extend into the cavernous sinus (Fig. 1). This lesion showed heterogeneous intensities on both T1-weighted (T1W) and T2-weighted (T2W) images and heterogeneous contrast enhancement on T1W gadolinium-enhanced images due to solid and cystic components with internal calcification and hemorrhage areas. Heterogeneous diffusion restriction areas were noted on diffusion-weighted images (DWI) and the ADC map, indicating high cellularity in the lesion. The mean ADC value of the solid tumor was $0.594 \times 10^{-3} \text{ mm}^2/\text{s}$, and the minimum ADC value was $0.460 \times 10^{-3} \text{ mm}^2/\text{s}$. The complete blood count and biochemistry were in the normal range. The chest radiograph and abdominal ultrasound showed no abnormalities.

A trigeminal schwannoma tumor diagnosis was made, and surgical resection was performed. Intraoperatively, a well-demarcated tumor was found in the left cerebellopontine angle. It mainly grew in the cisternal space involving the trigeminal nerve and infiltrated the middle cranial fossa. It also infiltrated the left cavernous sinus. Complete resection was impossible. Surgical resection was performed to the extent feasible.

The patient's postoperative course was uneventful. MRI 4 days postoperative (Fig. 2) showed an enlargement of the subarachnoid space in the left cerebellopontine angle and Meckel's cave, corresponding to the tumor bed level. Enhancing residual tumor was found in the lateral cavernous sinus wall. Diffusion restriction on the DWI with corresponding ADC

map and no enhancement at the left middle cerebellar peduncle and pons suggested ischemic lesions.

On microscopy, tumor cells were described as small round cells with a rounded nucleus, minimal cytoplasm, and finely granular chromatin with a high nuclear/cytoplasmic ratio (Fig. 3). They comprised a cluster of tumor cells surrounding a central region containing neuropil (Homer Wright rosettes). Periodic-acid Schiff (PAS) staining was negative. Tumor cells were positive for oligodendrocyte transcription factor 2 (OLIG2), CD99, and NESTIN and negative for SYNAP, CK, and CHRO (Fig. 3). All these features favored cerebral differentiating neuroblastoma.

The patient had an uneventful and good postsurgical recovery. They were discharged and required a follow-up examination postsurgery. Recurrence was detected on contrast-enhanced brain MRI scan in the next postsurgical follow-up (55 days after surgery), the recurrent tumor was proliferating and increasing in size ($55 \times 34 \text{ mm}$). Imaging showed a large mass in the left cerebellopontine angle, widespread through Meckel's cave and extending into the left middle cranial fossa. It also showed that the basilar artery was compressed, and the tumor enveloped the left internal carotid artery due to cavernous sinus invasion. Tumor volume and peritumoral edema contributed to the mass effect. The cerebellar peduncle, brainstem, and fourth ventricle were compressed and displaced to the right due to the risk of developing secondary obstructive hydrocephalus (Fig. 4). The follow-up images include of chest radiograph and abdominal ultrasound did not detected any

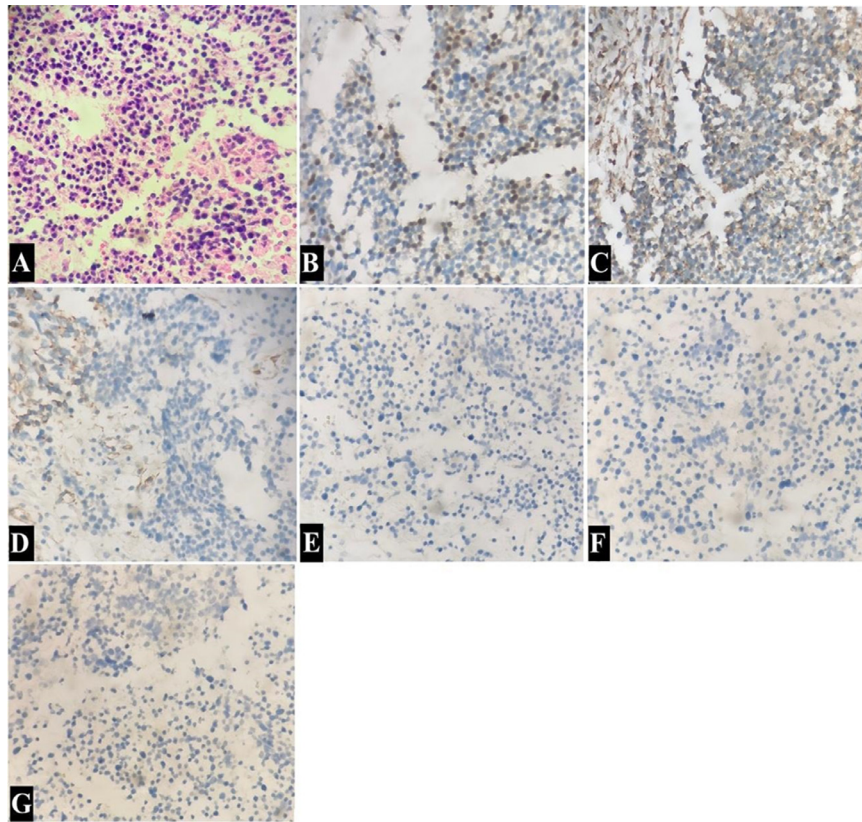


Fig. 3 – Histopathological images. (A) A microscopic histopathological image showing small round tumor cells arranged in sheets dispersed in the stroma (PAS staining; $\times 200$ magnification). Immunohistochemical staining of tumor cells ($\times 200$ magnification) for (B) OLIG2, (C) CD99, (D) NESTIN, (E) SYNAP, (F) CK, and (G) CHRO.

secondary lesions. Based on the patient's medical history, MRI and histological evidence supported a PCN-NB diagnosis. The patient was lost during follow-up because they transferred to a new treatment site.

Discussion

PCN-NB is a sporadic intracranial and spinal neuroblastoma manifestation that mostly affects neonates and adolescents [1,4,6,7]. PCN-NB was previously classified as a primitive neuroectodermal tumor, a group of intracranial neoplasms occurring in pediatrics with similar pathological characteristics, including pineoblastoma, ependyoblastoma, medulloblastoma, medulloepithelioma, and primary cerebral neuroblastoma [4,5,7,11]. However, with state-of-the-art histopathological investigations, the term was discontinued by WHO in 2016. The PCN-NB tumor is now classified with the ICD-O code 9500/3, a neuroepitheliomatous neoplasms category under neuronal and paraneuronal tumors [2,3]. Lu et al. [2] managed the SEER program for PCN-NB from 1973 to 2013, describing accompanying histopathological changes and delivering up-to-date representative and valuable statistics for PCN-NB, which remains one of the least understood malignant tumors of the CNS. This study reported that the annual prevalence of

PCN-NB had decreased from 0.28 to 0.12 cases per 1,000,000 population annually, most often involving neonates [2].

Neuroblastoma typically arises in primordial neural crest cells that naturally grow in the adrenal medulla and sympathetic nerve ganglia, explaining the tumor's behavior in several typical locations. An error in developing neural crest cells and the CNS gives a nearly closed door to generate PCN-NB [6]. This abnormal development of neural crest cells also explains why neuroblastoma is more common in children than adults [1,4,6,7]. The 2 most frequent histological PCN-NB subtypes are neuroblastoma and ganglioneuroblastoma [2,12]. There are 2 criteria for establishing a PCN-NB diagnosis: a histo-pathological appearance appropriate for neuroblastoma and no other systemic neuroblastoma. In the 2021 WHO classification of CNS tumors, PCN-NB was classified in the "Other CNS Embryonal Tumors" group [8]. PCN-NB generally has DNA methylation changes that activate the forkhead box R2 (FOXR2) gene, explaining the tumor's embryonal structure with small round cells and regions with differentiation of neuropil, neurolytic, and ganglion cells with uniform OLIG2 and neuronal antigen synaptophysin activation [6].

Previous studies claim that PCN-NB imaging characteristics are nonspecific and unrealizable for differentiating it from other intracranial malignant and benign neoplasms [6]. In addition to their unfamiliar middle cranial fossa-cerebellopontine angle location and nonspecific imaging fea-

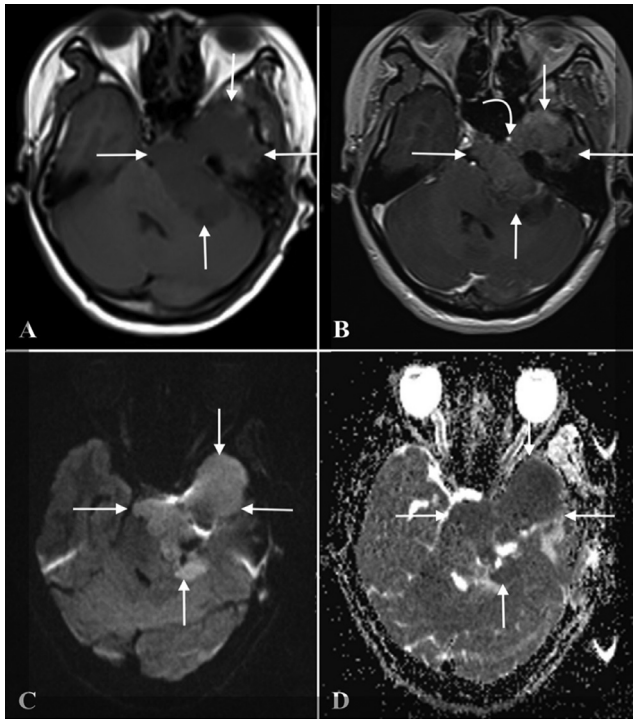


Fig. 4 – MRI brain images at 55 days postsurgery. (A) An axial precontrast T1W image showing a rapidly growing recurrent tumor in the left cerebellopontine angle (straight arrows) spreading through Meckel's cave and extending into the left middle cranial fossa, invading the cavernous sinus and surrounding the left internal carotid artery (curved arrow). The cerebellar peduncle, brainstem, and fourth ventricle were compressed and displaced to the right. (B) A postcontrast T1W image showing a contrast-enhancing lesion. The lesion with diffusion restriction appears (C) bright on DWIs and (D) dark on the ADC map.

tures, PCN-NBs generally occur sporadically in adults. Therefore, a preoperative PCN-NB diagnosis was impossible in our case. In this patient, both preoperative imaging diagnosis and intraoperative diagnoses were trigeminal schwannoma since the tumor extended from the cerebellopontine angle to Meckel's cave. Heterogeneous signals in MRI showed both solid and cystic components. The tumor also had a well-defined capsule, developed around the cranial trigeminal nerve, and the cavernous sinus was intact.

However, several MRI features in this case report did not support the preoperative diagnosis. First, the tumor showed significantly restricted diffusion on diffusion sequences both preoperative and at 55 days postoperative, suggesting a hypercellular tumor. Second, the tumor showed rapid local recurrent and aggressive features. A typical intracranial schwannoma is an extra-axial and benign neoplasm that usually shows slow expansion for tumors arising from Schwann cells encapsulating the cranial nerve, of which vestibular schwannoma is the most common, accounting for 70%–80% of cases, followed by cranial trigeminal nerve [13,14]. In pathology, intracranial schwannoma comprises heterogeneous regions of

2 cell types: small oval Antoni A cells with hypercellularity and dense stroma and Antoni B cells with loose stroma and hypocellularity. Therefore, it generally does not show restricted diffusion [11,14–16].

Tumors originating in the cerebellopontine angle-middle cranial fossa should be included in the differential diagnosis in the adult population. These include grade 1–3 meningiomas that account for 10%–15% of cases, benign tumors (eg, epidermoid cysts) that account for 5% of cases, cavernous sinus hemangiomas, and other malignant neoplasms such as brain metastasis, chondrosarcoma, chordoma, medulloblastoma that each account for only 1% of cases [14].

Meningioma is the most common extra-axial tumor type in adults and the second most frequent tumor in the cerebellopontine angle [11,14]. About 90% of meningiomas are benign, 9% are atypical, and 1% are malignant [14]. Meningiomas generally have an iso-to-hypo signal in the brain cortex in both T1W and an iso-hyper signal on T2W, with vivid enhancement with or without a dural tail [14]. Cystic meningiomas or malignant meningiomas (grade 2–3) occasionally show cystic degeneration with heterogeneous enhancement, and malignant meningiomas can sometimes show restricted diffusion in solid areas. In 2016, Era's Lucknow Medical College & Hospital in India [7] reported a case of a 6-year-old female with an aggressive extra-axial tumor in the frontal region, which had intra-tumoral cystic degeneration and restricted diffusion in solid areas. The patient underwent surgical excision with pathological confirmation of an extra-axial PCN-NB; no lesions in other organs were found.

An epidermoid cyst is the fourth most frequent tumor in the cerebellopontine angle. They are benign and show restricted diffusion but do not enhance after injection [14,17]. Differentiating them from other malignant tumors in the cerebellopontine angle, such as extra-axial medulloblastoma, atypical meningioma, chondrosarcoma, chordoma, or metastasis, is extremely challenging since they have similar imaging features and an overall frequency of only 1% [14]. In this case report, the highest priority diagnoses for this adult patient were an atypical meningioma, metastasis, or extra-axial medulloblastoma rather than neuroblastoma [14].

A promising variable that could support a neuroblastoma diagnosis is ADC. In our patients, the mean ADC value in the solid tumor region was $0.594 \times 10^{-3} \text{ mm}^2/\text{s}$, and the minimum ADC value was $0.460 \times 10^{-3} \text{ mm}^2/\text{s}$. These low ADC values are due to the tumor's hypercellularity that restricts the Brownian motion of water molecules [10]. This value is within the range of ADC values reported by Nina et al. [10] (mean: $0.81 \times 10^{-3} \text{ mm}^2/\text{s}$; range: $0.39\text{--}1.47 \times 10^{-3} \text{ mm}^2/\text{s}$) and higher than the ADC values they reported for ganglioneuromas and ganglioneuroblastomas (mean: $1.6 \times 10^{-3} \text{ mm}^2/\text{s}$; range: $1.13\text{--}1.99 \times 10^{-3} \text{ mm}^2/\text{s}$). In addition, Hung et al. [11] reported higher mean and minimum ADC values for schwannomas ($1.173 \times 10^{-3} \text{ mm}^2/\text{s}$ and $1.045 \times 10^{-3} \text{ mm}^2/\text{s}$) and cerebellopontine angle meningiomas ($0.841 \times 10^{-3} \text{ mm}^2/\text{s}$ and $0.716 \times 10^{-3} \text{ mm}^2/\text{s}$). Moreover, the mean ADC value for PCN-NBs is lower than that of other tumors showing restricted diffusion, such as epidermoid cysts ($1.197 \times 10^{-3} \text{ mm}^2/\text{s}$) [17], chondrosarcomas ($2.051 \times 10^{-3} \text{ mm}^2/\text{s}$), classic chordomas ($1.474 \times 10^{-3} \text{ mm}^2/\text{s}$), and poorly differentiated chordomas ($0.875 \times 10^{-3} \text{ mm}^2/\text{s}$) [18].

Overall, PCN-NB prognoses are poor and depend on the patient's age, tumor extension, and tumor location [6]. Metastatic disease of PCN-NB is high and accounts for 40% of cases [6]. Therefore, all patients with known PCN-NBs should be examined to detect brain-vertebral and cerebrospinal fluid metastasis [6]. Surgical excision is the treatment of choice for PCN-NBs. However, Lu et al. [2] advocated radiotherapy as a supportive PCN-NB treatment.

Conclusions

PCN-NB is a rare neoplasm often affecting neonates and adolescents that was categorized under neuroepitheliomatous tumors by WHO in 2016. Therefore, few studies have explored its imaging characteristics, treatment protocol, and prognosis. We reported a case with a PCN-NB in the middle cranial fossa-cerebellopontine angle with MRI features and histopathological characteristics with potential differential diagnoses. Diagnosing brain tumors and PCN-NBs should rely on a comprehensive evaluation of epidemiology, age, conventional and advanced imaging characteristics, and histopathological features.

Author's contributions

Bui QH and Nguyen DH contributed equally to this article as first authorship. Bui QH and Nguyen DH: Case file retrieval and case summary preparation. Nguyen DH and Nguyen MD: preparation of manuscript and editing. All authors read and approved the final manuscript.

Availability of data and materials

Data and materials used and/or analyzed during the current study are available from the corresponding author on reasonable request.

Ethics approval and consent to participate

Our institution does not require ethical approval for reporting individual cases or case series.

Patient consent

Informed consent for patient information to be published in this article was obtained.

REFERENCES

- [1] Borni M, Znazen M, Mdhaflar N, Boudawara MZ. A rare case of pediatric primary central nervous system differentiating neuroblastoma: an unusual and rare intracranial primitive neuroectodermal tumor (a case report). *Pan Afr Med J* 2021;40:33. doi:10.11604/pamj.2021.40.33.30587.
- [2] Lu X, Zhang X, Deng X, Yang Z, Shen X, Sheng H, et al. Incidence, treatment, and survival in primary central nervous system neuroblastoma. *World Neurosurg* 2020;140:e61–72. doi:10.1016/j.wneu.2020.04.145.
- [3] Louis DN, Perry A, Reifenberger G, von Deimling A, Figarella-Branger D, Cavenee WK, et al. The 2016 World Health Organization Classification of Tumors of the Central Nervous System: a summary. *Acta Neuropathol* 2016;131(6):803–20. doi:10.1007/s00401-016-1545-1.
- [4] Hart MN, Earle KM. Primitive neuroectodermal tumors of the brain in children. *Cancer* 1973;32(4):890–7. doi:10.1002/1097-0142(197310)32:4<890::aid-cnrcr2820320421>3.0.co;2-o.
- [5] Horten BC, Rubinstein LJ. Primary cerebral neuroblastoma. A clinicopathological study of 35 cases. *Brain* 1976;99(4):735–56. doi:10.1093/brain/99.4.735.
- [6] Mishra R, Agrawal A, Mishra R, Agrawal A. Primary central nervous system neuroblastoma: an enigmatic entity. London, England: IntechOpen; 2021. doi:10.5772/intechopen98244.
- [7] Gupta P, Mehrotra S, Kumar A, Srivastara AN. Primary cerebral neuroblastoma: an unusual intracranial PNET with neuronal differentiation. *IJAR* 2016;4:230–8. doi:10.21474/IJAR01/643.
- [8] Osborn AG, Louis DN, Poussaint TY, Linscott LL, Salzman KL. The 2021 World Health Organization classification of tumors of the central nervous system: what neuroradiologists need to know. *AJNR Am J Neuroradiol* 2022;43(7):928–37. doi:10.3174/ajnr.A7462.
- [9] Tietze A, Mankad K, Lequin MH, Ivarsson L, Mirsky D, Jaju A, et al. Imaging characteristics of CNS neuroblastoma-FOXR2: a retrospective and multi-institutional description of 25 cases. *Am J Neuroradiol* 2022;43(10):1476–80. doi:10.3174/ajnr.A7644.
- [10] Gahr N, Darge K, Hahn G, Kreher BW, von Buiren M, Uhl M. Diffusion-weighted MRI for differentiation of neuroblastoma and ganglioneuroblastoma/ganglioneuroma. *Eur J Radiol* 2011;79(3):443–6. doi:10.1016/j.ejrad.2010.04.005.
- [11] Nguyen DH, Le TD, Nguyen DM, Nguyen HK, Ngo DK, Duong DH, et al. Diagnostic performance of quantitative signal intensity measurements on magnetic resonance imaging for distinguishing cerebellopontine angle meningioma from acoustic schwannoma. *Eur Rev Med Pharmacol Sci* 2022;26(19):7115–24. doi:10.26355/eurrev_202210_29897.
- [12] Shimada H, Ambros IM, Dehner LP, Hata J, Joshi VV, Roald B, et al. The International Neuroblastoma Pathology Classification (the Shimada system). *Cancer* 1999;86(2):364–72.
- [13] Ortega-Merchan MP, Reyes F, Mejía JA, Rivera DM, Galvis JC, Marquez JC. Cystic trigeminal schwannomas. *Radiol Case Rep* 2019;14(12):1513–17. doi:10.1016/j.radcr.2019.09.031.
- [14] Renowden S. Imaging of the cerebello-pontine angle. *Pract Neurol* 2014;14(5):e2. doi:10.1136/practneurol-2014-000949.
- [15] Skolnik AD, Loevner LA, Sampathu DM, Newman JG, Lee JY, Bagley LJ, et al. Cranial nerve schwannomas: diagnostic imaging approach. *Radiographics* 2016;36(5):1463–77. doi:10.1148/rg.2016150199.
- [16] Bozdag M, Er A, Ekmekci S. Diagnostic efficacy of signal intensity ratio and apparent diffusion coefficient

- measurements in differentiating cerebellopontine angle meningioma and schwannoma. *Erciyes Med J* 2020;42(3):281–8. doi:[10.14744/etd.2020.61580](https://doi.org/10.14744/etd.2020.61580).
- [17] [Chen S, Ikawa F, Kurisu K, Arita K, Takaba J, Kanou Y. Quantitative MR evaluation of intracranial epidermoid tumors by fast fluid-attenuated inversion recovery imaging and echo-planar diffusion-weighted imaging. *AJNR Am J Neuroradiol* 2001;22\(6\):1089–96.](#)
- [18] Yeom KW, Lober RM, Mobley BC, Harsh G, Vogel H, Allagio R, et al. Diffusion-weighted MRI: distinction of skull base chordoma from chondrosarcoma. *AJNR Am J Neuroradiol* 2013;34(5):1056–61 S1. doi:[10.3174/ajnr.A3333](https://doi.org/10.3174/ajnr.A3333).